

Role of Organic Cation Transporter 1, OCT1 in the Pharmacokinetics and Toxicity of *cis*-Diammine(pyridine)chloroplatinum(II) and Oxaliplatin in Mice

Shuanglian Li · Ying Chen · Shuzhong Zhang · Swati S. More · Xiaozhu Huang · Kathleen M. Giacomini

Received: 8 September 2010 / Accepted: 25 October 2010 / Published online: 23 November 2010
© The Author(s) 2010. This article is published with open access at Springerlink.com

ABSTRACT

Purpose The goal of this study was to test the hypothesis that by controlling intracellular uptake, organic cation transporter 1, Oct1 is a key determinant of the disposition and toxicity of *cis*-diammine(pyridine)chloroplatinum(II)(CDPCP) and oxaliplatin.

Methods Pharmacokinetics, tissue accumulation and toxicity of CDPCP and oxaliplatin were compared between *Oct1*^{-/-} and wild-type mice.

Results After intravenous administration, hepatic and intestinal accumulation of CDPCP was 2.7-fold and 3.9-fold greater in *Oct1* wild-type mice ($p < 0.001$). Deletion of Oct1 resulted in a significantly decreased clearance (0.444 ± 0.039 l/min*kg versus 0.649 ± 0.0807 l/min*kg in wild-type mice, $p < 0.05$) and volume distribution (1.90 ± 0.16 l/kg versus 3.37 ± 0.196 l/kg in wild-type mice, $p < 0.001$). Moreover, Oct1 deletion resulted in more severe off-target toxicities in CDPCP-treated mice. Histologic examination of the liver and measurements of liver function indicated that the level of hepatic toxicity was mild and reversible, but was more apparent in the wild-type mice. In contrast, the effect of Oct1 on the pharmacokinetics and toxicity of oxaliplatin in the mice was minimal.

Conclusions Our study suggests that Oct1 plays an important role in the pharmacokinetics, tissue distribution and toxicity of CDPCP, but not oxaliplatin.

KEY WORDS OCT1 · pharmacokinetics · platinum agent · toxicity · transporter

ABBREVIATIONS

ABC	ATP Binding Cassette
CDPCP	<i>cis</i> -Diammine(pyridine)chloroplatinum(II)
FBS	fetal bovine serum
GAPDH	glyceraldehydes-3-phosphate dehydrogenase
ICP-MS	inductively coupled plasma mass spectrometry
ITS	insulin-transferrin-selenium
Kim-1	kidney injury molecule-1
MPP ⁺	N-methylquinine, and 1-methyl-4-phenylpyridinium
OCTs	organic cation transporters
PK	pharmacokinetics
qRT-PCR	quantitative real-time polymerase chain reaction
SLC	solute carrier
TEA	tetraethylammonium

INTRODUCTION

Membrane transporters play important roles in drug disposition and response (1–5). Recently, organic cation transporter 1 (OCT1), encoded by *SLC22A1*, has been shown to affect the pharmacokinetics and pharmacodynamics of the anti-diabetic drug, metformin (6,7). In humans, OCT1 is primarily expressed in the liver (8–10), whereas in rodents, Oct1 is expressed in equal abundance in the liver, kidney, and small intestine (11,12). In general, the human OCT1 mediates intracellular uptake of a broad range of structurally diverse monovalent organic cations with molecular weights of less than 400 Daltons (13,14). Substrates of OCT1 include endogenous compounds, such as choline, creatinine, and monoamine neurotransmitters; clinically used drugs, such as metformin, oxaliplatin and

S. Li · Y. Chen · S. Zhang · S. S. More · K. M. Giacomini (✉)
Department of Bioengineering and Therapeutic Sciences
University of California
1550 4th Street
San Francisco, California 94158, USA
e-mail: kathy.giacomini@ucsf.edu

X. Huang
Lung Biology Center, University of California
San Francisco, California 94143, USA

cimetidine; and a variety of xenobiotics, such as tetraethylammonium (TEA, model cation), N-methylquinine, and 1-methyl-4-phenylpyridinium (MPP⁺) (13,15,16). *In vivo*, *Oct1*^{-/-} mice display impaired liver uptake and intestinal excretion of a subset of organic cations, such as TEA, MPP⁺, and metformin (4,6,17), suggesting that the transporter Oct1 is important for the uptake of certain xenobiotics and drugs into various tissues, including the liver in the animal model.

Platinum-based chemotherapies have been widely used to treat solid tumors since the 1970s (18). Although cisplatin is effective against several solid tumors, its clinical use is limited because of its toxic effects as well as the intrinsic and acquired resistance of some tumors to this drug (19). To overcome limitations related to toxicities and resistance, other platinum agents have been developed (20). Oxaliplatin, approved in 2002 for the treatment of colorectal cancer in combination with 5-FU/leucovorin (21), exhibits a different pattern of sensitivity to that of cisplatin in the NCI60-cell human tumor panel, and in combination with 5-FU/leucovorin produces response rates twice that of 5-FU/leucovorin regimens alone in the treatment of colorectal cancer, against which cisplatin is inactive (20,22,23). Moreover, compared with cisplatin, oxaliplatin shows a more favorable toxicity profile.

Cis-diammine(pyridine)chloroplatinum(II) (CDPCP), belongs to a different series of platinum analogues from cisplatin, carboplatin and oxaliplatin. In particular, it is a cationic triamine complex that possesses desirable physical properties, such as high stability and solubility in aqueous media. Although CDPCP violates some of the classical structure-activity relationship, its anti-cancer activity was established in murine tumor models (24). However, CDPCP has never been tested in humans, possibly because this compound only forms monofunctional complexes with DNA, and due to its polarity, the drug was not expected to cross cell membrane readily (25). A recent study, however, showed that CDPCP can largely escape repair, yet inhibit transcription very effectively, and its adducts should persist longer than those of cisplatin yet produce a similar number of downstream consequences that might raise the therapeutic potential of CDPCP relative to cisplatin (25).

Recently, we showed that CDPCP is an excellent substrate of OCT1 (25). When overexpressed in transfected cells, OCT1 substantially increased the cellular uptake and cytotoxicity of CDPCP, suggesting that OCT1 facilitates intracellular accumulation of CDPCP, thereby sensitizing the cells to CDPCP cytotoxicity. Our *in vitro* studies also indicated that OCT1 facilitates the accumulation of oxaliplatin, though the effect was much smaller in comparison to CDPCP (15,25). Currently, there is an increased interest in further developing CDPCP as an anti-cancer

drug regarding the high selectivity of CDPCP for cells expressing hOCT1 and/or hOCT2, which are broadly expressed in human liver, kidney and human colorectal cancer (8–10,13,15).

In this study, we determined the pharmacokinetics and toxic properties of CDPCP and oxaliplatin in mice and tested the hypothesis that Oct1 plays a major role in the pharmacokinetics and toxicities of these drugs using *Oct1*^{-/-} mice. Specifically, we examined the role of Oct1 in the pharmacokinetics, tissue accumulation and toxicities of CDPCP and oxaliplatin in *Oct1*^{-/-} and wild-type mice. Our results demonstrate that Oct1 plays an important role not only in the pharmacokinetics of CDPCP, but also in its toxicities. However, the role of Oct1 in the pharmacokinetics of oxaliplatin was proven to be minimal. Our study sets the stage for further preclinical and clinical studies of CDPCP.

MATERIALS AND METHODS

Drugs and Reagents

Oxaliplatin and disopyramide were purchased from Sigma (St. Louis, MO). ITS (Insulin-Transferrin-Selenium) was purchased from Invitrogen (Carlsbad, CA). CDPCP was synthesized in our laboratory as described below. Solutions of oxaliplatin (5 mM) and CDPCP (10 mM) were freshly prepared in saline or PBS. The stock solutions were stored frozen at -20°C and discarded after 1 month of preparation. The cell culture media DMEM H21 medium, William's E, heat-inactivated fetal bovine serum (FBS), and L-glutamine were purchased from the Cell Culture Facility of the University of California, San Francisco (San Francisco, CA).

Synthesis of CDPCP

CDPCP was synthesized by a method adapted from Hollis *et al.* (24). Briefly, to a solution of cisplatin (900 mg, 3 mmol) in 15 mL of anhydrous DMF, AgNO₃ (485 mg, 2.85 mmol) was added at room temperature, and the mixture was allowed to stir for 24 h. The resulting precipitate of AgCl was removed by filtration before the addition of pyridine (242 µL, 3 mmol) to the filtrate. After the solution was stirred for an additional day, the DMF was removed under vacuum, and the remaining oil was triturated with CH₂Cl₂ (100 mL), followed by trituration with diethyl ether (50 mL). The resulting solid was filtered and then recrystallized from hot methanol to obtain product *cis*-[Pt(NH₃)₂(Pyr)Cl](NO₃) as a light yellow solid (yield 720 mg, 1.77 mmol, 59%). ¹H NMR (400 MHz, D₂O) δ8.90 (m, 1H, Ar), 8.45 (m, 2H, Ar), 7.31 (m, 2H,

Ar), 4.72, 4.26 (bs, 3H, NH_3); ESI-MS 343.1 $[M]^+$; Elemental Analysis: Found (%) C, 15.12; H, 2.50; N, 13.62. Calculate for $C_5H_{11}ClN_4O_3Pt$ (%): C, 14.80; H, 2.73; N, 13.81.

Cell Lines and Transfection

Human embryonic kidney (HEK) 293 cells stably transfected with the full-length reference human OCT1 cDNA (HEK-hOCT1) and with the empty vector (HEK-MOCK) were established previously in our laboratory (6,15). HEK293 cells stably transfected with pcDNA5/FRT vector (Invitrogen) containing the full-length reference mouse Oct1 cDNA (HEK-mOct1) were established using Lipofectamine 2000 (Invitrogen) per manufacturer's instructions. The stable clones were selected with 75 μ g/ml hygromycin B.

Primary Mouse Hepatocytes

Primary hepatocytes were isolated from *Oct1*^{+/+} and *Oct1*^{-/-} mice by the UCSF Liver Center using the standard collagenase method (26). For the CDPCP uptake assay, the isolated primary hepatocytes were seeded onto collagen-coated 6-well plates (Becton Dickinson, Bedford, MA) at a density of 0.8×10^6 cells/well in culture medium. After attachment (2–3 h), the cells were maintained in fresh medium for another 16–24 h followed by drug treatment as described below. For the uptake of oxaliplatin, the freshly isolated hepatocytes in suspension (1.5×10^5 cells/tube) instead of attached cells were used. During the incubation, the suspended cells were mixed several times by gentle vortex.

Cell Culture

The culture medium for stably transfected cells was DMEM H21 medium supplemented with 10% FBS, 100 units/ml penicillin and 100 μ g/ml streptomycin and 60 μ g/ml hygromycin B. The culture medium for primary hepatocytes was William's E medium supplemented with 100 units/ml penicillin, 100 μ g/ml streptomycin, 10% fetal bovine serum (FBS), 0.1 μ M dexamethasone, 2 mM L-glutamine, 1X ITS (100X ITS from Invitrogen). All cell lines were grown at 37°C in a humidified atmosphere with 5% CO_2 .

Cellular Accumulation of Platinum

The cellular accumulation of platinum was determined as described previously (15) with some modifications. Briefly, the cells were incubated in serum-free culture medium containing the indicated platinum compounds with or

without a specific inhibitor at 37°C in 5% CO_2 for 1 h unless specified. After incubation, cells were washed with ice-cold PBS three times. Then the cells were dissolved in 100 μ l of 70% nitric acid at 65°C for at least 2.5 h. Distilled water containing 10 ppb of iridium (Sigma) and 0.1% Triton X-100 was added to the samples to dilute nitric acid to 7%. The platinum content was measured by inductively coupled plasma mass spectrometry (ICP-MS) in the Analytical Facility at the University of California at Santa Cruz (Santa Cruz, CA). Cell lysates from a set of identical cultures were used for BCA protein assay. Cellular platinum accumulation was normalized to the protein content.

Platinum-DNA Adduct Formation

The platinum content associated with genomic DNA was determined as described previously (15) with some modifications. Briefly, the cells were incubated in the serum-free culture medium containing platinum drugs with or without an OCT1 inhibitor at 37°C in 5% CO_2 for 1 h unless specified. After incubation, cells were washed three times with ice-cold PBS. Genomic DNA was isolated from the cells using Wizard Genomic DNA Purification kit (Promega, Madison, WI) according to the manufacturer's protocol. The DNA-bound platinum was determined by ICP-MS. The DNA content from the same DNA preparation was measured by absorption spectroscopy at 260 nm. Platinum-DNA adduct level was normalized to total DNA content.

RNA Isolation

Total RNA from primary hepatocytes was isolated using an RNeasy Mini kit (Qiagen, Valencia, CA) according to the manufacturer's protocols. Total RNA from tissues was extracted using Trizol (Invitrogen). During the RNA purification procedure, DNase I was treated to digest residual genomic DNA. RNA was quantified spectrophotometrically at 260 nm. Extracted RNA was stored at $-80^\circ C$ until use.

Quantitative Real-Time PCR

Five μ g of total RNA from each sample was reverse transcribed into cDNA using a superscript first-strand cDNA synthesis kit (Invitrogen, Carlsbad, CA) according to the manufacturer's protocol. Quantitative real-time PCR (qRT-PCR) was carried out in a 96-well plate in a total volume of 10 μ l reaction solution which includes a cDNA equivalent of 2 μ g total RNA, specific probe and Taqman Universal Master Mix (Applied Biosystems, Foster City, CA). The thermal cycling conditions (ABI Prism 7700) were

95°C for 20 s followed by 40 cycles of 95°C for 3 s and 60°C for 30 s. The amplification of glyceraldehydes-3-phosphate dehydrogenase (GAPDH) mRNA was used as an internal control.

Animals

Oct1^{-/-} mice were generated as described elsewhere (6). The animals used in all experiments were in FVB background and were age-matched *Oct1*^{-/-} and *Oct1*^{+/+} (wild-type) mice between 8 and 10 weeks of age. All animals were housed in a virus-free, temperature-controlled facility on a 12-h light-dark cycle. Mice were allowed standard mouse food and water *ad libitum*. All experiments on mice were approved by the Institutional Animal Care and Use Committee of University of California at San Francisco and carried out according to the “Principles of Laboratory Animal Care” (NIH publication #85-23, revised in 1985).

Tissue Accumulation Studies in Mice

Eight-week-old male *Oct1*^{+/+} and *Oct1*^{-/-} mice were given platinum drugs in saline via tail vein injection. The animals were sacrificed at different time points after treatment. Blood samples were collected by heart puncture and transferred into heparinized BD vacutainer blood collection tubes. Blood was centrifuged for 30 min at 1000 x g, and the plasma was decanted and frozen at -80°C until analysis. Tissues (liver, kidney, heart, lung, brain, intestine, spleen and muscle) were collected as quickly as possible and snap frozen in liquid nitrogen. Five µl of plasma and about 10–30 mg of tissues were used for total platinum measurement by ICP-MS.

Pharmacokinetics Study in Mice

Eight-week-old male *Oct1*^{+/+} and *Oct1*^{-/-} mice were given platinum drugs in saline via tail vein injection and placed in metabolic cages for 24 h. Blood samples (20 µl) were collected at different time points by tail vein bleeding into heparinized micro-hematocrit capillary tubes (Fisher, Pittsburg, PA). Blood was centrifuged for 5 min using Microhematocrit Centrifuge (Thermo Fisher Scientific Inc. Waltham, MA), and the plasma was decanted and frozen at -80°C until analysis. Urine was collected from tubes attached to the cages. Tissues (liver, kidney, intestine, muscle) were collected as quickly as possible upon the last time point and snap frozen in liquid nitrogen. Five µl of plasma, urine and about 10–30 mg of tissues were used for total platinum measurement by ICP-MS. The pharmacokinetics parameters were obtained by two-compartmental

analysis using WinNonlin 4.0 (Pharsight Corporation, Mountain view, CA).

Toxicity Study in Mice

Eight-week-old male *Oct1*^{-/-} and *Oct1*^{+/+} mice were randomized and treated with saline or platinum drugs via tail vein injection (CDPCP) or i.p. injection (oxaliplatin) once weekly for a total of 3 weeks (CDPCP) or once daily for a total of 5 days (oxaliplatin). The animals were closely monitored and sacrificed when they became moribund. Body weight was monitored and recorded. All surviving animals were sacrificed 24 h after the last treatment. On the day of the terminal sacrifice, the animals were anesthetized with isoflurane, and blood (500–1000 µl) was collected by heart puncture and centrifuged for 30 min at 1000 X g at 4°C. The serum was frozen at -80°C until analysis. Tissues (liver, kidney, intestine, and muscle) were collected and divided into two halves: one half of the tissues were fixed in 4% paraformaldehyde for histopathology examination, and the other half of the tissues were snap frozen in liquid nitrogen.

Hematological Evaluation

The whole blood (50–100 µl) was placed in K2EDTA coated tubes, and complete blood count (CBC) tests were conducted within 6 h by Mouse Pathology Core of UCSF Helen Diller Family Comprehensive Cancer Center.

Clinical Chemistry Evaluation

Alaninetransaminase (ALT), aspartatetransaminase (AST), alkaline phosphatase (ALKP), total protein, albumin, glucose, blood urea nitrogen (BUN), creatinine and electrolytes in serum were measured by the Clinical Laboratory of the San Francisco General Hospital.

Histopathological Examination

The tissues (liver, intestine and kidney) fixed in 4% paraformaldehyde were embedded in paraffin, cut into thin sections and mounted on glass slides. The tissue sections were stained with hematoxylin and eosin for microscopic examination.

Statistical Analysis

Unless specified, data are expressed as mean ± standard deviation (SD). Data were analyzed statistically using the unpaired Student's *t*-test and Fisher exact test according to the sample size. Multiple comparisons were performed with Dunnett's two-tailed test after one-way ANOVA. A *p* value of less than 0.05 was considered statistically significant.

RESULTS

Platinum Uptake in Cells Over-Expressing hOCT1 and mOct1 After Exposure to CDPCP and Oxaliplatin

As shown in Fig. 1a, we observed that the uptake of platinum in HEK-mOct1 transfected cells exposed to CDPCP (10 μ M) (1470 \pm 66.6 pmol/mg protein/hr) was 53-fold greater than that in HEK-MOCK cells (27.4 \pm 7.43 pmol/mg protein/hr) (p <0.001). This effect was slightly greater than the effect of hOCT1 on platinum uptake after exposure to CDPCP (10 μ M) (852 \pm 135 pmol/mg protein/hr). The effect of hOCT1 and mOct1 on the cellular uptake of oxaliplatin was much smaller than on CDPCP uptake, and, again, mOct1, in comparison to hOCT1, promoted a greater uptake of platinum in cells exposed to oxaliplatin (p <0.001; Fig. 1b).

Intracellular Platinum Uptake and DNA Adduct Formation of Platinum Drugs in Primary Mouse Hepatocytes

To examine the role of Oct1 in the disposition of CDPCP in the liver, we compared the intracellular uptake and DNA adduct formation of CDPCP in hepatocytes derived from *Oct1* wild-type mice with that in hepatocytes derived from *Oct1*^{-/-} mice. The studies showed that the hepatocellular uptake of CDPCP (10 μ M) after 1 hr exposure in hepatocytes from *Oct1* wild-type mice (251 \pm 94.6 pmol/mg protein/hr) was 2.9-fold of that in hepatocytes from *Oct1*^{-/-} mice (87.8 \pm 7.61 pmol/mg protein/hr) (p <0.01; Fig. 2a). Co-incubation of CDPCP with disopyramide (150 μ M), an Oct1 inhibitor, resulted in a 4.5-fold decrease in the platinum uptake in hepatocytes from *Oct1* wild-type mice (control *versus* disopyramide-treated, 251 \pm 94.6 pmol/mg protein/hr *versus* 55.9 \pm 1.41 pmol/mg protein/hr) (p <0.01) with no effect in hepatocytes from *Oct1*^{-/-} mice (control *versus* disopyramide-

treated, 87.8 \pm 7.61 pmol/mg protein/hr *versus* 95.8 \pm 17.6 pmol/mg protein/hr) (p >0.05; Fig. 2a). The platinum-DNA adduct level after 1 h exposure to CDPCP in hepatocytes from *Oct1* wild-type mice (0.0857 \pm 0.0232 pmol/ μ g DNA) was 2.4-fold greater than that in hepatocytes from *Oct1*^{-/-} mice (0.0351 \pm 0.00344 pmol/ μ g DNA) (p <0.01; Fig. 2b). Co-incubation of CDPCP with disopyramide (150 μ M) significantly decreased (3.7-fold; p <0.01) platinum-DNA adduct formation in hepatocytes from *Oct1* wild-type mice (control *versus* disopyramide treated, 0.0857 \pm 0.0232 pmol/ μ g DNA *versus* 0.0233 \pm 0.00847 pmol/ μ g DNA) (p <0.01) with no effect in hepatocytes from *Oct1*^{-/-} mice (control *versus* disopyramide-treated, 0.0351 \pm 0.00344 pmol/ μ g DNA *versus* 0.0338 \pm 0.00798 pmol/ μ g DNA) (p >0.05; Fig. 2b). Collectively, data shown in Fig. 2a and b suggest that Oct1 mediates the uptake and binding to DNA of CDPCP in mouse hepatocytes.

For oxaliplatin, the intracellular uptake rate of platinum increased proportionally with increasing concentrations of oxaliplatin in hepatocytes isolated from both *Oct1*^{+/+} and *Oct1*^{-/-} mice (Fig. 2c and d). In all hepatocytes isolated from *Oct1*^{+/+} and *Oct1*^{-/-} mice, the intracellular uptake rate of oxaliplatin was similar between 30 min exposure and 120 min exposure. Compared to hepatocytes isolated from *Oct1*^{-/-} mice, hepatocytes isolated from *Oct1*^{+/+} mice had significantly higher platinum uptake rate after incubation with 1 μ M and 5 μ M of oxaliplatin for 30 min and 120 min. The hepatocellular uptake rate of oxaliplatin after 30 min exposure in hepatocytes from *Oct1* wild-type mice (1 μ M *versus* 5 μ M, 1.54 \pm 0.300 pmol/mg protein/hr *versus* 5.55 \pm 0.384 pmol/mg protein/hr) was 1.8-fold and 1.4-fold of that in hepatocytes from *Oct1*^{-/-} mice (1 μ M *versus* 5 μ M, 0.855 \pm 0.184 pmol/mg protein/hr *versus* 3.97 \pm 0.500 pmol/mg protein/hr), respectively (p <0.05; Fig. 2c). Similar results were obtained after 120 min of exposure (Fig. 2d). These data indicate that Oct1 is likely to play a role in facilitating the transport of oxaliplatin across

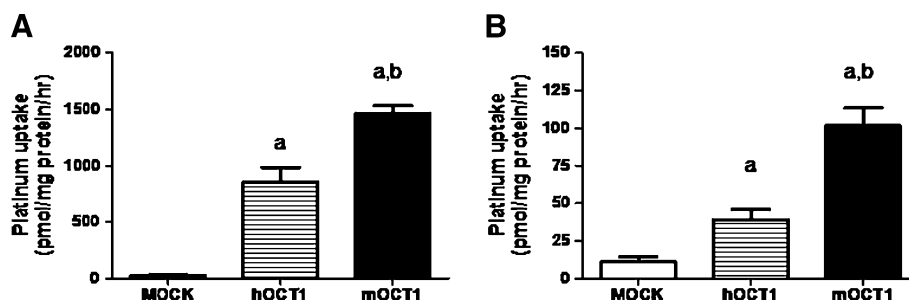
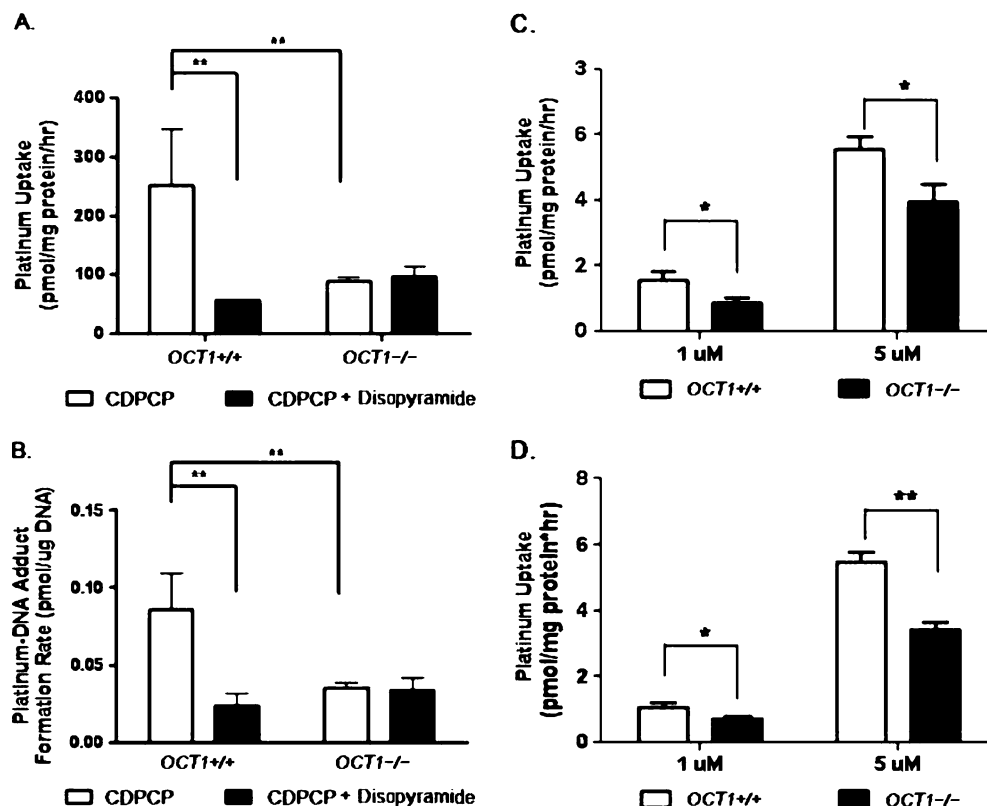


Fig. 1 Intracellular uptake of platinum after 1-h exposure to platinum drugs in cells over-expressing hOCT1 and mOct1. The cellular uptake of platinum in hOCT1-transfected (striped bar), mOct1-transfected (solid bar) cells and in the corresponding MOCK (white bar) cells after incubation with CDPCP (A) and oxaliplatin (B) were determined as described in Materials and Methods. Briefly, the cells were incubated in serum-free culture medium containing CDPCP (10 μ M) or oxaliplatin (10 μ M) at 37°C and 5% CO₂ for 1 h. Total platinum concentration inside the cells was determined using ICP-MS. Total platinum concentration was normalized to protein content. Data are presented as the mean \pm SD (n =6). a: significantly greater than in MOCK cells (P <0.001); b: significantly greater than in hOCT1-transfected cells (P <0.001).

Fig. 2 Effect of Oct1 on the intracellular uptake of platinum in primary mouse hepatocytes after exposure to CDPCP and oxaliplatin. Intracellular platinum uptake (A) and platinum-DNA adduct formation (B) after 1 h exposure to 10 μ M CDPCP in the absence (white bars) or presence (black bars) of an Oct1 inhibitor, disopyramide (150 μ M) and intracellular platinum uptake after 30 min (C) and 120 min (D) exposure to 1 μ M and 5 μ M of oxaliplatin in hepatocytes from *Oct1* wild-type (white bars) and *Oct1*^{-/-} mice (black bars) were determined as described in Materials and Methods. Total platinum concentration inside the cells and DNA-bound platinum was determined using ICP-MS. Total platinum concentration was normalized to protein content, and DNA-bound platinum was normalized to DNA content. Data are presented as the mean \pm SD ($n=3$) and from a representative experiment. * $P<0.05$, ** $P<0.005$.



hepatocytes. However, the effect of Oct1 on oxaliplatin uptake is less than its effect on CDPCP uptake.

Tissue Accumulation of Platinum After Treatment with Platinum Drugs in *Oct1* Wild-Type and *Oct1*^{-/-} Mice

To extend the *in vitro* cellular studies, we examined the role of Oct1 in the accumulation of platinum drugs in various tissues after dosing to *Oct1* wild-type and *Oct1*^{-/-} mice (Fig. 3). The tissue accumulation study of CDPCP (8 mg/kg) showed that total levels of platinum in the plasma 1 h after CDPCP treatment were significantly higher (1.3-fold) in *Oct1*^{-/-} mice than in *Oct1* wild-type mice (Fig. 3a, $p<0.001$). Comparing the absolute platinum level in various tissues (Table 1 and Fig. 3a), we observed that the platinum accumulation levels in liver and intestine were significantly higher in *Oct1* wild-type mice than in *Oct1*^{-/-} mice ($p<0.01$). However, the platinum accumulation levels in kidney, heart and skeletal muscle in *Oct1* wild-type mice were significantly lower than in *Oct1*^{-/-} mice ($p<0.05$). When the absolute platinum level in the various tissues was normalized to the corresponding plasma concentration (Table 1 and Fig. 3b), we observed that platinum levels in the muscle and kidney were no longer significantly different between *Oct1* wild-type and *Oct1*^{-/-} mice ($p>0.05$), while the normalization to plasma concentration had no effect on the platinum

accumulation level in the heart ($p<0.01$). The normalized platinum accumulation was 2.7-fold greater in the liver of *Oct1* wild-type compared to the knockout mouse and 3.9-fold greater in the intestine of *Oct1* wild-type compared to knockout mice. The highest platinum accumulation levels were found in liver and intestine in both *Oct1* wild-type and *Oct1*^{-/-} mice (Table 1). Taken together, this study suggests that the expression of Oct1 in liver and intestine contributes to the enhanced accumulation of CDPCP in these organs.

The effect of OCT1 on the tissue distribution of oxaliplatin was first examined 6 h after intravenous dosing of oxaliplatin (8 mg/kg). The absolute platinum levels and the platinum levels normalized to plasma platinum concentrations in various tissues including liver, kidney, intestine, spleen, bone marrow and muscle showed no significant difference between *Oct1*^{+/+} and *Oct1*^{-/-} mice ($p>0.05$). The effect of Oct1 on the tissue distribution of oxaliplatin was reexamined after a shorter treatment duration. After 1 h treatment with oxaliplatin (8 mg/kg), the plasma concentration of oxaliplatin in *Oct1*^{+/+} was slightly but significantly lower than that in *Oct1*^{-/-} mice (*Oct1*^{+/+} versus *Oct1*^{-/-}, 5.96 ± 0.54 μ M versus 6.69 ± 0.62 μ M; $p<0.05$; Fig. 3c). Comparing the oxaliplatin accumulation in various tissues, we observed that the absolute oxaliplatin levels in intestine, kidney and heart in *Oct1*^{-/-} mice were significantly higher than in *Oct1*^{+/+} mice (Fig. 3c; $p<0.05$). However, after normalization with corresponding plasma

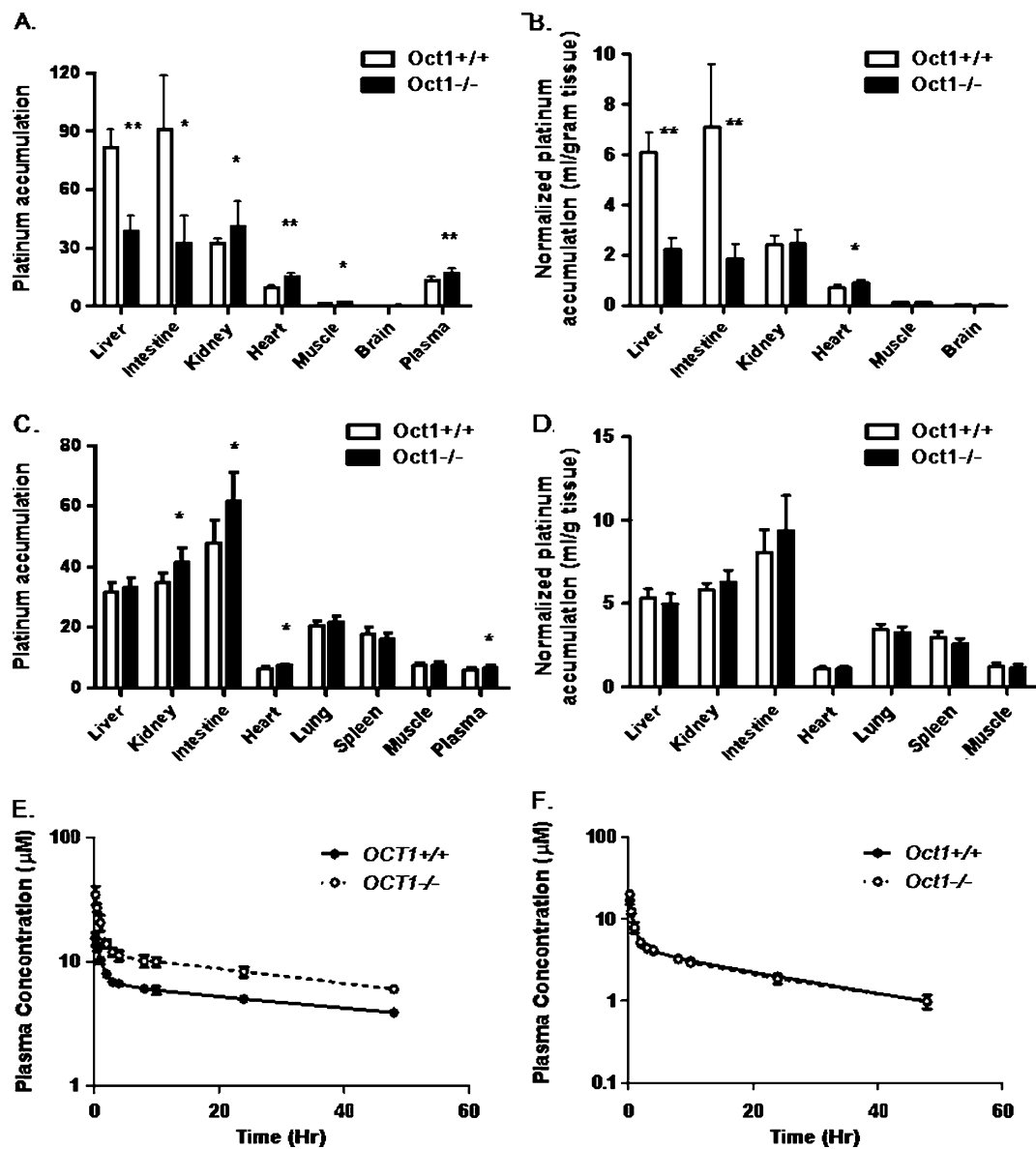


Fig. 3 Effects of Oct1 on tissue accumulation of platinum drugs and plasma concentrations after intravenous dosing of CDPCP and oxaliplatin in mice. Absolute platinum accumulation levels (**A**, **C**), normalized platinum accumulation levels (**B**, **D**) in various tissues were measured 1 h post dosing of 8 mg/kg of CDPCP (**A**, **B**) and oxaliplatin (**C**, **D**), respectively in *Oct1*-wild-type and *Oct1*^{-/-} mice. Plasma concentrations of CDPCP (**E**), oxaliplatin (**F**) in *Oct1*-wild-type and *Oct1*^{-/-} mice were measured at 15, 30 min, 1, 2, 3, 4, 8, 10, 24, 48 hr after i.v. dosing of CDPCP (8 mg/kg) and oxaliplatin (8 mg/kg). The platinum levels in plasma and various organs were determined using ICP-MS. The unit for tissue accumulation of platinum is nmol/gram tissue, the unit for plasma is μM (**A**, **C**). Data are presented as the mean \pm SD * $P < 0.05$; ** $P < 0.001$.

concentrations, the differences in renal, cardiac, and intestinal accumulation between *Oct1*^{+/+} and *Oct1*^{-/-} mice were not observed (Fig. 3d).

Platinum accumulation in various tissues was also measured at the end of pharmacokinetics studies, i.e. 48 h after dosing. The effects of Oct1 on the tissue accumulation of platinum drugs were similar to the data obtained at 1 h for both CDPCP and oxaliplatin, i.e. Oct1 enhanced the hepatic and intestinal accumulation of CDPCP, and exerted insignificant effect on the oxaliplatin accumulation.

Pharmacokinetics of Platinum Drugs in *Oct1* Wild-Type and *Oct1*^{-/-} Mice

The time-course of platinum in plasma following a single i.v. dose of CDPCP (8 mg/kg) to *Oct1* wild-type and *Oct1*^{-/-} mice is shown in Fig. 3e. Similar to the pharmacokinetics of AMD473 (picoplatin), a third-generation platinum agent, which is currently in Phase-III clinical trials for treatment of non-small-cell lung cancer (NSCLC) (27,28), the concentration versus time course of total platinum followed a two-

Table 1 Platinum Accumulation in Various Tissues 1 h After IV Administration of CDPCP (8 mg/kg) in *Oct1+/+* (n = 5) and *Oct1-/-* (n = 7) Mice

	Plasma (μM)		Liver		Kidney		Intestine		Muscle		Heart		Brain	
	Absolute (pmol/g tissue)	Normalized (ml/g tissue)	Absolute (pmol/g tissue)	Normalized (ml/g tissue)	Absolute (pmol/g tissue)	Normalized (ml/g tissue)	Absolute (pmol/g tissue)	Normalized (ml/g tissue)	Absolute (pmol/g tissue)	Normalized (ml/g tissue)	Absolute (pmol/g tissue)	Normalized (ml/g tissue)	Absolute (pmol/g tissue)	Normalized (ml/g tissue)
<i>Oct1</i> WT	13.5 ± 1.72	6.09 ± 0.792	32.1 ± 2.93	2.40 ± 0.374	90.9 ± 28.0	7.13 ± 2.47	1.62 ± 0.144	0.121 ± 0.0118	9.77 ± 1.20	0.725 ± 0.0747	0.436 ± 0.116	0.0328 ± 0.0114		
<i>Oct1</i> KO	17.2 ± 2.11	2.23 ± 0.440	44.3 ± 11.5	2.47 ± 0.552	32.3 ± 14.2	1.84 ± 0.571	2.08 ± 0.292	0.122 ± 0.0201	15.4 ± 1.83	0.898 ± 0.0813	0.487 ± 0.128	0.0282 ± 0.00518		
<i>Oct1</i> WT/ KO	0.8**	2.1**	0.7*	1.0	2.8*	3.9**	0.8*	1.0	0.6**	0.8*	0.9	1.2		

Total platinum in plasma and tissues was determined by ICP-MS. Normalized platinum levels in various tissues were obtained by dividing the total platinum levels by plasma concentration. Data are expressed as the mean ± SD.

* $p < 0.05$; ** $p < 0.001$.

compartment model in both *Oct1* wild-type and *Oct1-/-* mice. The mean plasma concentrations of CDPCP in *Oct1-/-* mice were significantly higher than that in *Oct1* wild-type mice at all time points (Fig. 3e). The mean pharmacokinetics parameters are shown in Table 2. Comparing the pharmacokinetics parameters of CDPCP in *Oct1* wild-type mice with *Oct1-/-* mice, we observed that the plasma platinum exposure over 48 hrs (AUC_{0-48}) in *Oct1-/-* mice was 1.69-fold of that in *Oct1* wild-type mice ($p < 0.01$), and the volume of distribution of CDPCP in *Oct1* wild-type mice was 1.77-fold of that in *Oct1-/-* mice ($p < 0.01$). Moreover, a significantly greater total clearance was observed in *Oct1* wild-type mice in comparison to *Oct1-/-* mice ($p < 0.05$), although renal clearance showed no difference between *Oct1+/+* mice and *Oct1-/-* mice. The renal clearance contributed to about 50% of the total clearance of platinum from plasma in both *Oct1+/+* and *Oct1-/-* mice.

Consistent with the pharmacokinetics of CDPCP and the previous report of oxaliplatin pharmacokinetics in rats (29), the concentration versus time course of total platinum following i.v. administration of oxaliplatin (8 mg/kg) exhibited a biexponential decline in both *Oct1* wild-type and *Oct1-/-* mice (Fig. 3f). The pharmacokinetics parameters were not significantly different between *Oct1+/+* and *Oct1-/-* mice, as shown in Table 3. The clearance and volume of distribution of oxaliplatin in both *Oct1+/+* and *Oct1-/-* mice were similar to that reported in BD2F1 mice (30).

Toxicity Study of CDPCP in *Oct1* Wild-Type and *Oct1-/-* Mice

Based on the results of the dose-range finding toxicity study that CDPCP at 90 mg/kg and above resulted in significant changes in body weight, liver-to-body-weight ratio, liver function and hematology, we selected doses between 90 mg/kg and 120 mg/kg for use in evaluating the role of Oct1 in CDPCP toxicity. The role of Oct1 in toxicity of CDPCP was determined by comparing the toxicity profile of CDPCP between *Oct1+/+* and *Oct1-/-* mice. The dose of CDPCP started with 120 mg/kg, which later was reduced to 90 mg/kg due to death or moribundity observed in *Oct1-/-* mice at 120 mg/kg.

CDPCP Resulted in Much Greater Body Weight Loss in *Oct1-/-* Mice

Compared with saline control group, CDPCP treatment caused body weight loss in both *Oct1+/+* and *Oct1-/-* mice (Fig. 4a). However, the body weight loss was much greater in *Oct1-/-* mice than in *Oct1+/+* mice. The greater decrease in body weight in *Oct1-/-* mice treated with

Table 2 Plasma Platinum Pharmacokinetic Parameters Following a Single IV Administration of CDPCP (8 mg/kg) in *Oct1*+/+ and *Oct1*-/-mice (3 Per Group)

	<i>Oct1</i> +/+ Mean ± SD	<i>Oct1</i> -/ Mean ± SD	<i>Oct1</i> -/ <i>Oct1</i> +/+	P value
AUC ₀₋₄₈ (μM*hr)	257 ± 7.10	434 ± 29.4	1.69	0.009
AUC _{inf} (μM*hr)	604 ± 70.9	878 ± 74.4	1.45	0.009
CL (ml/min*kg)	0.649 ± 0.0807	0.444 ± 0.0391	0.68	0.017
CL _R (ml/min*kg)	0.320 ± 0.246	0.221 ± 0.177	0.69	0.603
V _{SS} (L/kg)	3.37 ± 0.196	1.90 ± 0.161	0.56	0.0006
C _{max} (μM)	17.9 ± 2.21	43.1 ± 7.68	2.41	0.005
T _{1/2,α} (hr)	0.639 ± 0.0324	0.494 ± 0.137	0.77	0.37
T _{1/2,β} (hr)	66.6 ± 9.75	48.3 ± 6.84	0.73	0.20

Blood samples for pharmacokinetic analysis were drawn up to 48 h. The pharmacokinetic parameters were obtained by two compartmental analysis using WinNonlin 4.0.

T_{1/2,α}, distribution half life; T_{1/2,β}, terminal half life; C_{max}, maximal plasma concentration; AUC_{inf}, area under the curve of plasma concentration from time 0 to infinity; V_{SS}, volume of distribution at steady state; CL, clearance; CL_R, renal clearance.

CDPCP was consistent with the higher plasma platinum concentration in these mice ($p < 0.005$; Fig. 6a).

Hepatic Toxicity of CDPCP was Enhanced in *Oct1*+/+ Mice

The liver-to-body-weight ratio was significantly increased compared to saline control in both *Oct1*+/+ and *Oct1*-/- mice (Fig. 4b). However, the liver-to-body-weight ratio change in *Oct1*+/+ mice, which was 28.8% increase in CDPCP-treated mice compared with saline-treated mice, was more striking than that in *Oct1*-/- mice, which was 14.7% increase in CDPCP-treated mice compared with saline-treated mice. To exclude the confounding effect of less body weight decrease in *Oct1*+/+ mice on the liver-to-body-weight ratio, the actual

liver weights between *Oct1*+/+ and *Oct1*-/- mice treated with CDPCP and saline were also compared. Our data showed that the actual liver weight was increased by CDPCP treatment in *Oct1*+/+ mice but not in *Oct1*-/- mice (CDPCP versus saline: 1.23 g versus 0.973 g in *Oct1*+/+ mice, $p < 0.00001$; 1.02 g versus 1.00 g in *Oct1*-/- mice, $p > 0.05$), indicating that CDPCP indeed resulted in hepatomegaly in *Oct1*+/+ mice. Moreover, CDPCP resulted in significant decrease in total serum protein levels and significant increase in glucose levels in *Oct1*+/+ mice, but not in *Oct1*-/- mice (Fig. 4c, d). However, the activities of ALT, AST and ALKP were not affected by CDPCP in either *Oct1*+/+ or *Oct1*-/- mice (Fig. 4e).

Histopathological examination of liver from *Oct1*-/- mice treated with either saline or CDPCP showed no clear signs

Table 3 Plasma Platinum Pharmacokinetic Parameters Following a Single iv Administration of Oxaliplatin (8 mg/kg) in *Oct1*+/+ and *Oct1*-/-Mice (3 Per Group)

	<i>Oct1</i> +/+ Mean ± SD	<i>Oct1</i> -/ Mean ± SD	<i>Oct1</i> -/ <i>Oct1</i> +/+	P value
AUC ₀₋₄₈ (μM*hr)	118.7 ± 4.37	118.5 ± 7.74	1.00	> 0.05
AUC (μM*hr)	147 ± 5.86	144 ± 16.0	0.98	> 0.05
CL (ml/min*kg)	2.29 ± 0.0916	2.35 ± 0.270	1.03	> 0.05
CL _R (ml/min*kg)	0.789 ± 0.267	1.09 ± 0.581	1.43	> 0.05
V _{SS} (L/kg)	3.80 ± 0.0950	3.56 ± 0.168	0.94	> 0.05
C _{max} (μM)	23.9 ± 3.39	30.4 ± 4.35	1.28	> 0.05
T _{1/2,α} (hr)	0.374 ± 0.0372	0.332 ± 0.0772	0.89	> 0.05
T _{1/2,β} (hr)	20.6 ± 0.818	19.2 ± 2.42	0.93	> 0.05

Blood samples for pharmacokinetic analysis were drawn up to 48 h. The pharmacokinetic parameters were obtained by two compartmental analysis using WinNonlin 4.0.

T_{1/2,α}, distribution half life; T_{1/2,β}, terminal half life; C_{max}, maximal plasma concentration; AUC_{inf}, area under the curve of plasma concentration from time 0 to infinity; V_{SS}, volume of distribution at steady state; CL, clearance; CL_R, renal clearance.

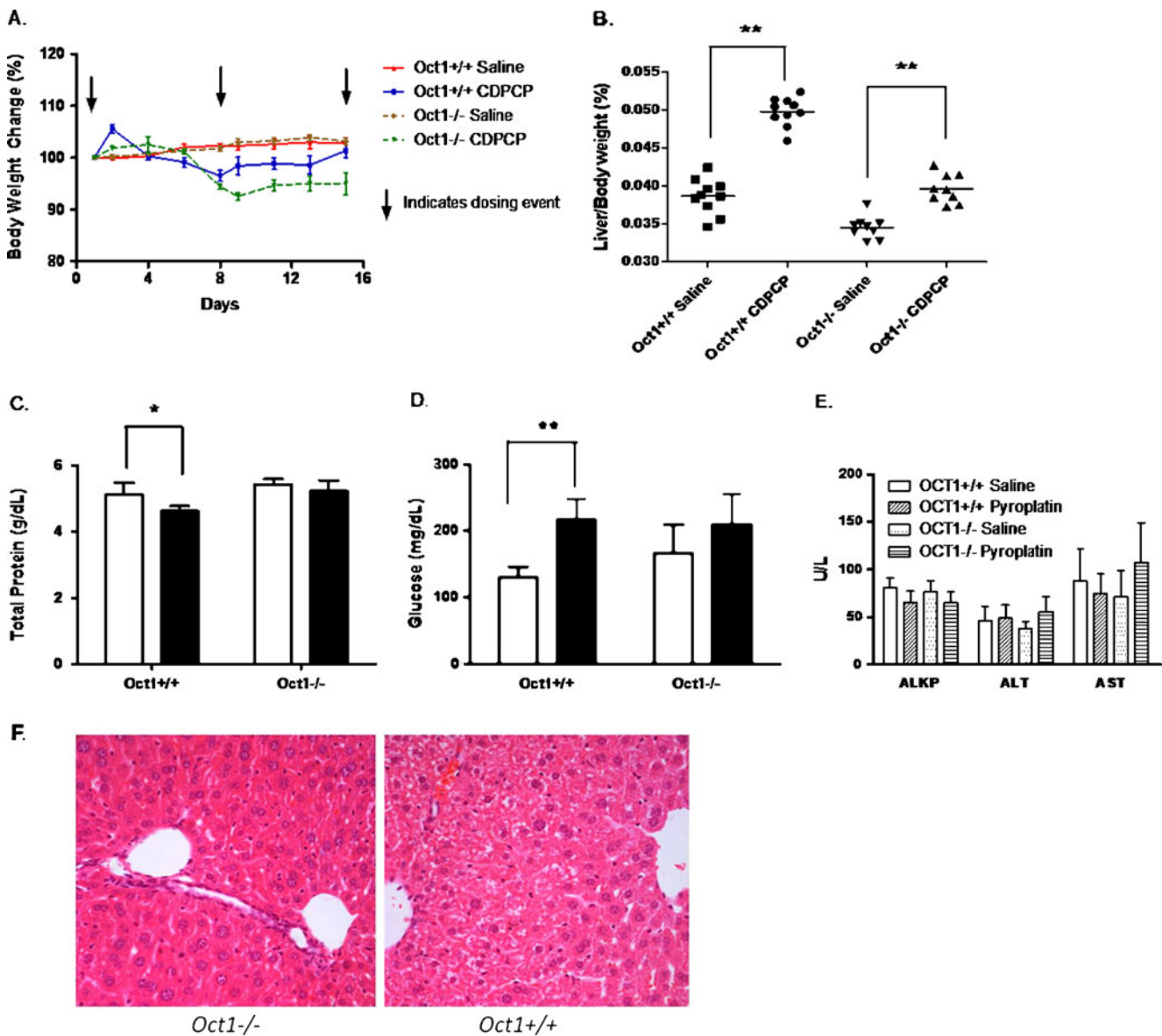


Fig. 4 Effects of Oct1 on body weight loss and liver toxicities of CDPCP in mice. *Oct1*^{-/-} and *Oct1*^{+/+} mice were treated with saline or CDPCP via tail vein injection once weekly for a total 3 weeks (at least 9 animals per group). The mice were fasted for at least 16 h before sacrifice. Body weight (**A**) was monitored three times per week. Blood and various tissues were collected 24 hrs after the last dose; liver weight was measured. Liver to body weight ratios (**B**), total protein levels in serum (**C**), glucose levels in serum (**D**) and activities of liver enzymes (**E**), were compared among groups. Liver histopathology (**F**) was examined; the magnification is 40X. Data are presented as the mean \pm SD ($n \geq 9$). * $P < 0.05$; ** $P < 0.001$.

of toxicity, while the liver from *Oct1*^{+/+} mice treated with CDPCP appeared to have enlarged and rounded hepatocytes, which are normally hexagonal (Fig. 4f). The irregular white spots, which were considered to be aqueous materials inside the hepatocytes pushed the nucleus aside, indicating CDPCP resulted in liver edema in *Oct1*^{+/+} mice. The hepatic lesion was more striking in the portal vein area than in other regions of the liver. Comparing the frequency and the severity of hepatic lesions, we observed that CDPCP caused more severe and frequent liver damage in *Oct1*^{+/+} mice in comparison to *Oct1*^{-/-} mice, as indicated by mild to moderate swollen hepatocytes (Table 4). The differences

did not reach statistical significance using Fisher exact test ($p = 0.07$), though trends were apparent. The greater hepatic toxicity in *Oct1*^{+/+} mice was consistent with the higher absolute hepatic platinum accumulation in these mice (Fig. 6b; $p < 0.005$). Further, at higher doses of CDPCP (120 mg/kg) used in our dose-finding studies, we observed significant increases in ALT in the wild-type, but not in the knockout, mice (data not shown). These data strongly suggest that *Oct1* deletion protects animals from developing liver toxicity and that *Oct1* plays a role not only in CDPCP disposition but also in CDPCP-associated organ toxicity.

Table 4 Histopathological Examination of Liver and Kidney in *Oct1*^{+/+} and *Oct1*^{-/-} Mice Following Repeated i.v. Doses of CDPCP

Genotype	Treatment	Liver	Kidney
OCT1 ^{+/+}	CDPCP	Severe swollen hepatocytes (3/4); Mild swollen hepatocytes(1/4)	Normal (4/4)
	Saline	Mild swollen hepatocytes(1/5)	Inflammation foci (1/5) Normal (5/5)
OCT1 ^{-/-}	CDPCP	Mild swollen hepatocytes(1/4)	Kidney tube protein contents (3/4); kidney hyaline necrosis (1/4)
	Saline	Multiple necrosis + inflammation foci (1/4)	Normal (4/4)

Livers and kidneys were harvested 24 hr following the third dose of CDPCP and fixed in 4% paraformaldehyde for histopathology examination. The denominator in the parenthesis represents the total number of animals that were examined. The numerator represents the number of animals that were affected.

Renal Toxicity of CDPCP was More Pronounced in *Oct1*^{-/-} Mice

In both *Oct1*^{+/+} and *Oct1*^{-/-} mice administered CDPCP, serum creatinine levels were not significantly different from mice administered saline ($p > 0.05$; Fig. 5a). Serum BUN levels were significantly reduced in CDPCP-treated *Oct1*^{+/+} mice compared with saline-treated *Oct1*^{+/+} mice ($p < 0.05$), while serum BUN was not affected by CDPCP in *Oct1*^{-/-} mice ($p > 0.05$; Fig. 5a). CDPCP treatment increased renal mRNA levels of Kim-1, a more sensitive and quantitative renal biomarker of early tubular damage, by

19.3-fold over control value in *Oct1*^{+/+} mice. However, the elevation of renal Kim-1 expression in *Oct1*^{-/-} mice following CDPCP treatment was much more striking than in *Oct1*^{+/+} mice; the fold difference over saline control was 117 (Fig. 5b).

Histologic evaluation of kidneys from CDPCP-treated mice demonstrated tubular cast formation, which was revealed by eosinophilic amorphous material and pyknotic and karyorrhectic debris (Fig. 5c.II) and degeneration of tubular cells, including tubular dilatation, tubular cell vacuolation, tubular cell detachment (Fig. 5c.III). The renal morphology change seemed to localize to the outer medulla

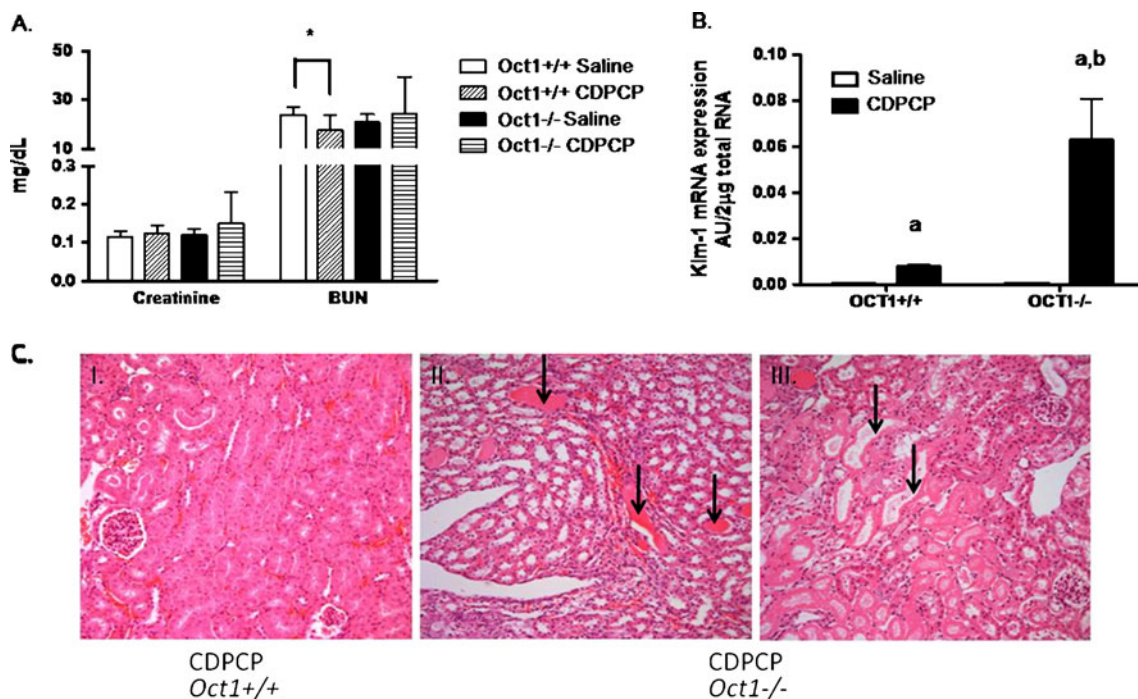


Fig. 5 Effect of Oct1 on renal toxicity of CDPCP in mice. *Oct1*^{-/-} and *Oct1*^{+/+} mice were treated with saline or CDPCP via tail vein injection once weekly for a total 3 weeks (at least 9 animals per group). The mice were fasted for at least 16 h before sacrifice. Blood and various tissues were collected 24 hrs after the last dose. Creatinine and BUN in serum (**A**) were measured. Total RNA from kidney was reverse-transcribed and the synthesized cDNA was subject to qRT-PCR using Kim-1 (**B**) probe. The amplification of glyceraldehydes-3-phosphate dehydrogenase (GAPDH) mRNA was used as an internal control. Kidney histopathology (**C**) was examined; the magnification is 20X; arrows indicate kidney lesions. Data are presented as the mean \pm SD. * $P < 0.05$; a: significantly greater than corresponding saline control groups ($P < 0.01$); b: significantly greater than *Oct1*^{+/+} mice ($P < 0.05$).

(Fig. 5c.II and c.III). Consistent with the Kim-1 expression study, the kidney tubular lesions were most prominent in *Oct1*^{-/-} mice treated with CDPCP compared with *Oct1*^{+/+} mice treated with CDPCP (Fig. 5c.I) and saline-treated control animals. The incidence and type of kidney lesion are listed in Table 4. We observed that CDPCP treatment resulted in a lower rate of kidney damage in *Oct1*^{+/+} mice than in *Oct1*^{-/-} mice, and the rate difference was marginally significant ($p=0.07$). The absolute renal platinum accumulation in *Oct1*^{-/-} mice was remarkably greater than that in *Oct1*^{+/+} mice (Fig. 6c; $p<0.05$). These data indicate that CDPCP is more toxic to the kidney in *Oct1*^{-/-} mice.

Toxicities of CDPCP in Other Sites

The hematological toxicity of CDPCP was more pronounced in *Oct1*^{-/-} mice, which was reflected by significant changes in white blood cell parameters, including neutrophil (%) and lymphocytes (%), and in platelet parameter, i. e. mean platelet volume (MPV), which were observed in CDPCP-treated *Oct1*^{-/-} mice but not in *Oct1*^{+/+} mice ($p<0.05$, data not shown). The higher plasma platinum concentration in *Oct1*^{-/-} mice supported greater hematological toxicity of CDPCP in these mice (Fig. 6a; $p<0.005$). Histological examination of intestine showed no signs of intestinal toxicity in either *Oct1*^{+/+} or *Oct1*^{-/-} mice following CDPCP treatment, although significantly higher intestinal accumulation of CDPCP in *Oct1*^{+/+} mice was observed (Fig. 6d, $p<0.05$).

Toxicity Study of Oxaliplatin in *Oct1* Wild-Type and *Oct1*^{-/-} Mice

To assess the role of Oct1 in the toxicities associated with oxaliplatin treatment, especially the hepatotoxicity, the *Oct1*^{+/+} and *Oct1*^{-/-} mice ($n=5$ per group) were treated with 6 mg/kg oxaliplatin or saline via i.p. injection once daily for a total of 5 days. Oxaliplatin caused more severe body weight loss in *Oct1*^{+/+} mice than in *Oct1*^{-/-} mice; the relative body weight loss in *Oct1*^{+/+} mice was 15.1%, whereas the relative body weight loss in *Oct1*^{-/-} mice was 6.8%. Although there was a significantly greater hepatic accumulation of oxaliplatin in *Oct1*^{+/+} mice, no difference was observed in liver size or activities of three liver-associated enzymes: ALT, AST and ALKP between *Oct1*^{+/+} and *Oct1*^{-/-} mice, respectively (data not shown). The liver histopathology examination showed no clear sign of liver damage associated with oxaliplatin treatment in either *Oct1*^{+/+} or *Oct1*^{-/-} mice. The data suggest that the hepatic toxicity of oxaliplatin observed in humans was not observed under the conditions used in this study, and a clear role for Oct1 in oxaliplatin-induced hepatotoxicity could not be established. The effect of Oct1 deletion on body weight was striking and suggests that Oct1 plays a role in the overall toxicity of oxaliplatin in the mice. Since oxaliplatin was not hepatotoxic under the conditions used in this study, we could not assess the effect of Oct1 on hepatotoxicity of oxaliplatin. The dosing regimen or dosing route used in our study might not be appropriate to elicit the hepatic toxicity.

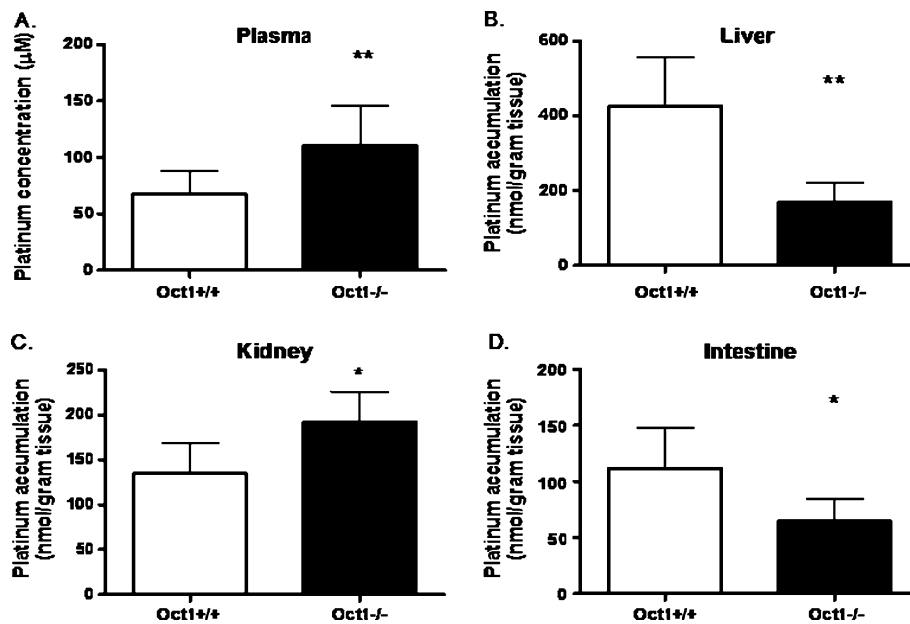


Fig. 6 Platinum concentrations in plasma and various tissues collected from the toxicity study. *Oct1*^{-/-} and *Oct1*^{+/+} mice were treated with saline or CDPCP via tail vein injection once weekly for a total 3 weeks (at least 9 animals per group). The mice were fasted for at least 16 h before sacrifice. Blood (A), liver (B), kidney (C), and intestine (D) were harvested 24 hrs after the last dose. Platinum was measured by ICP-MS. Data are presented as the mean \pm SD. * $P<0.05$; ** $P<0.005$.

Oct1 Deletion Resulted in Enhanced Expression of Oct2 and Oct3 in Various Tissues

mRNA levels of Oct2, Oct3, Ent1, Mate1 and Ctr1 in various tissues were determined by quantitative RT-PCR. The expression levels of Oct2 in liver was increased by 2.6-fold in *Oct1*^{-/-} mice compared with *Oct1*^{+/+} mice (Fig. 7a; $p < 0.05$). The increase of Oct2 expression in kidney and intestine of *Oct1*^{-/-} mice was 1.8- and 2.5-fold compared with *Oct1*^{+/+} mice, respectively. However, these changes did not reach statistical significance due to the relatively large variation (Fig. 7b, c; $p > 0.05$). The expression of Oct3 in liver in *Oct1*^{-/-} mice was 5.7-fold of that in *Oct1*^{+/+} mice (Fig. 7d, $p < 0.001$). There was no change in the expression levels of Ent1, Mate1 and Ctr1 in liver between *Oct1*^{+/+} mice and *Oct1*^{-/-} mice.

DISCUSSION

Though shown to be a potent anti-tumor platinum compound, CDPCP was never tested clinically. Because of its positive charge, the drug may have been thought to have poor pharmacokinetic characteristics. In recent studies, OCT1 was shown to play a role in the cellular uptake and consequent cytotoxicity of CDPCP in cell lines over-expressing OCT1 (25). Accordingly, we hypothesized that

OCT1 mediates the uptake of CDPCP *in vivo* in various tissues, particularly the intestine and liver, and that OCT1-mediated transmembrane flux may result in a favorable pharmacokinetic and toxicity profile for CDPCP. To test our hypothesis, we performed a comprehensive pharmacokinetic analysis using genetically modified *Oct1*^{-/-} mice in this study. The results suggest that deletion of Oct1 not only decreased the uptake of cellular platinum but also reduced the level of platinum-DNA adduct formation in hepatocytes after CDPCP exposure (Fig. 2). These results are in agreement with those in cells transfected with human OCT1 (25), although the fold difference in platinum levels between hepatocytes harvested from *Oct1*^{+/+} versus *Oct1*^{-/-} mice was much less than that between HEK293 cells over-expressing human OCT1 and control cells (25). These differences were not due to species differences between mOct1 and hOCT1, since our data suggest that CDPCP is a comparable or better substrate of mOct1 than of hOCT1 (Fig. 1). Drug-metabolizing enzymes and drug transporters normally are lost by liver cells in culture as a consequence of the adaptation of cells to the *in vitro* environment. Lecureu *et al.* reported that hepatocytes maintained in primary culture for several days were known to not only lose expression of albumin and cytochrome P-450 but also displayed low levels of OCT1 expression and activity (31). Studies from our laboratory also confirmed that the expression level of Oct1 in primary hepatocytes cultured from mouse liver was consid-

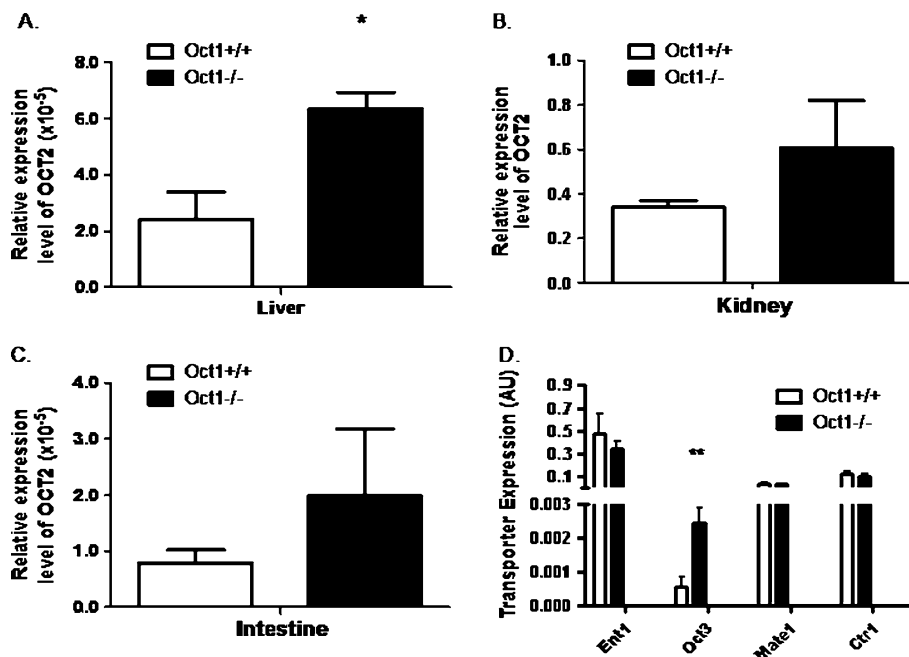


Fig. 7 Effects of *Oct1* deletion on the expression of Oct2 and Oct3 in various tissues in mice. The expression of Oct2 in liver (A), kidney (B) and intestine (C) and the expression of various drug transporters in liver (D) were determined by quantitative RT-PCR. Various tissues were harvested from age-matched *Oct1*^{+/+} and *Oct1*^{-/-} mice. Total RNA was extracted from these tissues and reverse-transcribed. The synthesized cDNA was subject to qRT-PCR using an Oct2, Ent1, Oct3, Mate1 and Ctr1 probes. The amplification of glyceraldehyde-3-phosphate dehydrogenase (GAPDH) mRNA was used as an internal control. Data are presented as the mean \pm SD ($n = 3$). * $P < 0.05$; ** $P < 0.001$.

erably lower than that in mouse liver (data not shown), suggesting that the isolation and culture procedures likely resulted in a reduced expression level of the Oct1 protein and therefore a reduction in the observed effect of Oct1 in the isolated hepatocytes.

The significantly higher hepatic and intestinal accumulation of CDPCP in *Oct1*^{+/+} mice was consistent with the abundance of Oct1 in liver and intestine of rodents (12,13). Normalization of tissue platinum levels to plasma concentrations of CDPCP excluded the effects of different plasma exposure on the uptake of CDPCP into the various tissues. Although there is strong Oct1 expression in the kidney of mice (12,13,32), it was notable that no differences were observed in the normalized levels of platinum in the kidneys of *Oct1*^{+/+} versus *Oct1*^{-/-} mice. This may be explained by the redundant function of Oct1/2 in the rodent kidney, and the Oct2 strongly expressed in the kidney can completely compensate for the loss of Oct1. Previously, CDPCP was shown to be a substrate of OCT2 (25). It is notable that enhanced expression of Oct2 and Oct3 in the liver of *Oct1*^{-/-} mice may have resulted in a reduction in the observed effect of Oct1 on CDPCP uptake in the liver (Fig. 7a and d).

Consistent with the high hepatic accumulation in *Oct1*^{+/+} mice, the hepatotoxicity of CDPCP was more prominent in these mice, as demonstrated by the increased liver-to-body-weight ratio, decreased total serum protein levels, increased serum glucose levels and histological changes at 90 mg/kg in the *Oct1* wild-type mice. The low BUN in the wild-type mice treated with CDPCP is also consistent with hepatotoxicity in these mice. A low BUN usually has little significance, but its causes include liver problems, malnutrition (insufficient dietary protein), or excessive alcohol consumption. Although there was greater hepatic toxicity in *Oct1*^{+/+} mice, the level of toxicity was considered mild and reversible. If CDPCP is developed as an anti-cancer drug, hepatic toxicity may not be a concern.

Recently, use of oxaliplatin has been associated with development of hepatic lesions, which include sinusoidal alteration, portal hypertension, increase in transaminases, gamma glutamyltranspeptidase and alkaline phosphatase, and steatohepatitis (6,33). In our study, the role of Oct1 in the tissue accumulation and the pharmacokinetics of oxaliplatin was proven to be minimal, and oxaliplatin was not hepatotoxic under the conditions used in this study. However, total plasma platinum levels may not reflect platinum complexes available for DNA and protein binding, anti-tumor effects and toxicity of the oxaliplatin. The fact that oxaliplatin administration resulted in a greater reduction in body weight in the wild-type mice in comparison to the *Oct1* knockout mice may suggest that Oct1 plays a role in the systemic toxicities of oxaliplatin.

In this study, we made an unexpected observation that *Oct1* deletion markedly increased the renal toxicity of CDPCP in *Oct1*^{-/-} mice, which was revealed by much greater Kim-1 mRNA expression level and histological changes of tubular cast formation and degeneration of tubular cells in *Oct1*^{-/-} mice (Fig. 5b, c.II, and c.III). The differential localization of organic cation transporters Oct1 and Oct2 in the basolateral membrane of rodent kidney proximal tubules may account for the greater kidney toxicity in *Oct1*^{-/-} mice. In particular, Oct1 was shown to be concentrated in the early proximal tubules in the renal cortex, whereas Oct2 was abundant in the late proximal tubules in the outer stripe of the outer medulla (34,35). In the report by Jonker *et al.* of the relative impact of Oct1 and Oct2 on the clearance of TEA (36), they observed that elimination of neither Oct1 nor Oct2 resulted in a decrease in renal TEA clearance, whereas elimination of both transporters eliminated TEA secretion. These data suggest that there is sufficient Oct1 transport capacity in the early renal proximal tubules to effectively clear the blood of substrate before it reaches the downstream Oct2-expressing cells of the late renal proximal tubules. CDPCP is an excellent substrate of both OCT1 and OCT2 (25). In *Oct1*^{-/-} mice, CDPCP will be secreted by Oct2-expressing cells in late renal proximal tubules. The greater exposure of the late proximal tubule to CDPCP may contribute to the enhanced toxicity of CDPCP observed in the *Oct1*^{-/-} mice. Further, Oct2 is likely to localize in the outer strip of the outer medulla and may produce a localized accumulation of CDPCP in this region. The outer medulla was the region most damaged by CDPCP (Fig. 5c.II and III).

The pharmacokinetics of CDPCP were consistent with the pharmacokinetics observed previously for oxaliplatin and picoplatin, suggesting that the drug has a pharmacokinetic profile similar to clinically used anti-cancer platinum agents. Deletion of Oct1 resulted in a reduction in the clearance and volume of distribution of CDPCP, which may be explained by the differences in the distribution of CDPCP to the tissues with high Oct1 expression, in particular, liver and intestine. The higher plasma platinum concentrations and AUC in *Oct1*^{-/-} mice in comparison to *Oct1*^{+/+} mice can be attributed to the lower clearance and volume of distribution in *Oct1*^{-/-} mice. Since the renal clearance of CDPCP was similar between *Oct1*^{+/+} and *Oct1*^{-/-} mice, the lower total clearance of CDPCP in the *Oct1*^{-/-} mice is likely due to a reduction in the uptake and subsequent covalent binding of CDPCP in the liver and intestine, organs that accumulate high levels of platinum.

Though other transporters may affect the disposition of CDPCP, this study clearly demonstrates that Oct1 plays a significant role in the pharmacokinetics of this drug. The lack of an important role of Oct1 in the pharmacokinetics of oxaliplatin may suggest a lower specificity of oxaliplatin

for Oct1 and that other transporters (or diffusion) may contribute to its tissue distribution and pharmacokinetics. In this study, CDPCP exhibited excellent pharmacokinetic properties, comparable to other clinically used platinum analogs. Moreover, CDPCP appears to possess a favorable toxicity profile, and Oct1 plays an important role in determining the toxicity profile of CDPCP. Our study supported the concept that by targeting drug influx transporters, off-target toxicities, such as renal, hematological toxicities, can be spared. Whether CDPCP can be used for targeted therapy of various cancers is worthy of further investigation. Further, this study provides another example of a drug distinct from metformin for which OCT1 may play a profound role in its pharmacokinetics and toxicities (4,6,7).

ACKNOWLEDGMENTS

This study was supported by a grant from the National Institutes of Health, GM36780 and a Grant from the TRDRP grant 17RT-0126. This work was also made possible in part by core service provided by UCSF liver center (NIH P30 DK26743). Y.C. was supported by National Research Service Award T32 GM07546 from the National Institutes of Health. We acknowledge the services provided by Mouse Pathology Core of UCSF Helen Diller Family Comprehensive Cancer Center, the J David Gladstone Histology and Microscopy core and the Clinical Laboratory of the San Francisco General Hospital. We also thank Rob Franks at the Institute of Marine Sciences of University of California, Santa Cruz, for his great help in analyzing platinum using ICP-MS.

Open Access This article is distributed under the terms of the Creative Commons Attribution Noncommercial License which permits any noncommercial use, distribution, and reproduction in any medium, provided the original author(s) and source are credited.

REFERENCES

1. Maeda K, Ieiri I, Yasuda K, Fujino A, Fujiwara H, *et al.* Effects of organic anion transporting polypeptide 1B1 haplotype on pharmacokinetics of pravastatin, valsartan, and temocapril. *Clin Pharmacol Ther.* 2006;79:427–39.
2. Hirano M, Maeda K, Shitara Y, Sugiyama Y. Drug-drug interaction between pitavastatin and various drugs via OATP1B1. *Drug Metab Dispos.* 2006;34:1229–36.
3. Chung J-Y, Cho J-Y, Yu K-S, Kim J-R, Oh D-S, *et al.* Effect of OATP1B1 (SLCO1B1) variant alleles on the pharmacokinetics of pitavastatin in healthy volunteers. *Clin Pharmacol Ther.* 2005;78:342–50.
4. Wang DS, Jonker JW, Kato Y, Kusuhashi H, Schinkel AH, *et al.* Involvement of organic cation transporter 1 in hepatic and intestinal distribution of metformin. *J Pharmacol Exp Ther.* 2002;302:510–5.
5. Lin JH, Yamazaki M. Clinical relevance of P-glycoprotein in drug therapy. *Drug Metab Rev.* 2003;35:417–54.
6. Shu Y, Sheardown SA, Brown C, Owen RP, Zhang SZ, *et al.* Effect of genetic variation in the organic cation transporter 1 (OCT1) on metformin action. *J Clin Invest.* 2007;117:1422–31.
7. Shu Y, Brown C, Castro RA, Shi RJ, Lin ET, *et al.* Effect of genetic variation in the organic cation transporter 1, OCT1, on metformin pharmacokinetics. *Clin Pharmacol Ther.* 2008;83:273–80.
8. Zhang L, Dresser MJ, Gray AT, Yost SC, Terashita S, *et al.* Cloning and functional expression of a human liver organic cation transporter. *Mol Pharmacol.* 1997;51:913–21.
9. Gorboulev V, Ulzheimer JC, Akhoundova A, Ulzheimer Teuber I, Karbach U, *et al.* Cloning and characterization of two human polyspecific organic cation transporters. *DNA Cell Biol.* 1997;16:871–81.
10. Su AI, Wiltshire T, Batalov S, Lapp H, Ching KA, *et al.* A gene atlas of the mouse and human protein-encoding transcriptomes. *Proc Natl Acad Sci USA.* 2004;101:6062–7.
11. Gruendemann D, Gorboulev V, Gambaryan S, Veyhl M, Koepsell H. Drug excretion mediated by a new prototype of polyspecific transporter. *Nature (London).* 1994;372:549–52.
12. Schweifer N, Barlow DP. The Lx1 gene maps to mouse chromosome 17 and codes for a protein that is homologous to glucose and polyspecific transmembrane transporters. *Mamm Genome.* 1996;7:735–40.
13. Jonker JW, Schinkel AH. Pharmacological and physiological functions of the polyspecific organic cation transporters: OCT1, 2, and 3 (SLC22A1-3). *J Pharmacol Exp Ther.* 2004;308:2–9.
14. Wright SH. Role of organic cation transporters in the renal handling of therapeutic agents and xenobiotics. *Toxicol Appl Pharmacol.* 2005;204:309–19.
15. Zhang SZ, Lovejoy KS, Shima JE, Lagpacan LL, Shu Y, *et al.* Organic cation transporters are determinants of oxaliplatin cytotoxicity. *Cancer Res.* 2006;66:8847–57.
16. Yonezawa A, Masuda S, Yokoo S, Katsura T, Inui K. Cisplatin and oxaliplatin, but not carboplatin and nedaplatin, are substrates for human organic cation transporters (SLC22A1-3 and multidrug and toxin extrusion family). *J Pharmacol Exp Ther.* 2006;319:879–86.
17. Jonker JW, Wagenaar E, Mol C, Buitelaar M, Koepsell H, *et al.* Reduced hepatic uptake and intestinal excretion of organic cations in mice with a targeted disruption of the organic cation transporter 1 (Oct1 [Slc22a1]) gene. *Mol Cell Biol.* 2001;21:5471–7.
18. Wong E, Giandomenico CM. Current status of platinum-based antitumor drugs. *Chem Rev.* 1999;99:2451–66.
19. Weiss RB, Christian MC. New cisplatin analogs in development—a review. *Drugs.* 1993;46:360–77.
20. Kelland L. The resurgence of platinum-based cancer chemotherapy. *Nat Rev Cancer.* 2007;7:573–84.
21. Ibrahim A, Hirschfeld S, Cohen MH, Griebel DJ, Williams GA, *et al.* FDA drug approval summaries: oxaliplatin. *Oncologist.* 2004;9:8–12.
22. Misset JL, Bleiberg H, Sutherland W, Bekradda M, Cvitkovic E. Oxaliplatin clinical activity: a review. *Crit Rev Oncol Hematol.* 2000;35:75–93.
23. Rixe O, Ortuzar W, Alvarez M, Parker R, Reed E, *et al.* Oxaliplatin, tetraplatin, cisplatin, and carboplatin: Spectrum of activity in drug-resistant cell lines and in the cell lines of the national cancer institute's anticancer drug screen panel. *Biochem Pharmacol.* 1996;52:1855–65.
24. Hollis LS, Amundsen AR, Stern EW. Chemical and biological properties of a new series of Cis-diammineplatinum(II) antitumor

- agents containing 3 nitrogen donors—Cis-[Pt(NH₃)₂(N-Donor Cl)]⁺. *J Med Chem.* 1989;32:128–36.
25. Lovejoy KS, Todd RC, Zhang SZ, McCormick MS, D'Aquino JA, *et al.* cis-diammine(pyridine)chloroplatinum(II), a monofunctional platinum(II) antitumor agent: Uptake, structure, function, and prospects. *Proc Natl Acad Sci USA.* 2008;105:8902–7.
 26. Moldeus P, Hogberg J, Orrenius S. Isolation and Use of Liver Cells. Fleischer S, Packer L, editors. *Methods in Enzymology, Vol. Lii. Biomembranes. Part C: Biological Oxidations Microsomal, Cytochrome P-450, and Other Hemoprotein Systems.* Xxii + 595p. Illus. Academic Press, Inc.: New York, N.Y., USA; London, England. Isbn 0-12-181952-3:60-71; 1978.
 27. Raynaud FI, Boxall FE, Goddard PM, Valenti M, Jones M, *et al.* cis-aminedichloro(2-methylpyridine)platinum(II) (AMD473), a novel sterically hindered platinum complex: *In vivo* activity, toxicology, and pharmacokinetics in mice. *Clin Cancer Res.* 1997;3:2063–74.
 28. More SS, Li S, Yee SW, Chen L, Xu Z, *et al.* Organic cation transporters modulate the uptake and cytotoxicity of picoplatin, a third-generation platinum analogue. *Mol Cancer Ther.* 2010;9:1058–69.
 29. Luo FR, Wyrick SD, Chaney SG. Pharmacokinetics and biotransformations of oxaliplatin in comparison with ormaplatin following a single bolus intravenous injection in rats. *Cancer Chemother Pharmacol.* 1999;44:19–28.
 30. Rice JR, Gerberich JL, Nowotnik DP, Howell SB. Preclinical efficacy and pharmacokinetics of AP5346, a novel diaminocyclohexane-platinum tumor-targeting drug delivery system. *Clin Cancer Res.* 2006;12:2248–54.
 31. Lecreur V, Guillouzo A, Fardel O. Differential expression of the polyspecific drug transporter OCT1 in rat hepatocarcinoma cells. *Cancer Letters.* 1998;126:227–33.
 32. Koepsell H. Polyspecific organic cation transporters: their functions and interactions with drugs. *Trends Pharmacol Sci.* 2004;25:375–81.
 33. Rubbia-Brandt L, Audard V, Sartoretti P, Roth AD, Brezault C, *et al.* Severe hepatic sinusoidal obstruction associated with oxaliplatin-based chemotherapy in patients with metastatic colorectal cancer. *Ann Oncol.* 2004;15:460–466.
 34. Sugawara-Yokoo M, Urakami Y, Koyama H, Fujikura K, Masuda S, *et al.* Differential localization of organic cation transporters rOCT1 and rOCT2 in the basolateral membrane of rat kidney proximal tubules. *Histochem Cell Biol.* 2000;114:175–80.
 35. Urakami Y, Okuda M, Masuda S, Akazawa M, Saito H, *et al.* Distinct characteristics of organic cation transporters, OCT1 and OCT2, in the basolateral membrane of renal tubules. *Pharm Res.* 2001;18:1528–34.
 36. Jonker JW, Wagenaar E, van Eijl S, Schinkel AH. Deficiency in the organic cation transporters 1 and 2 (Oct1/Oct2 [Slc22a1/Slc22a2]) in mice abolishes renal secretion of organic cations. *Mol Cell Biol.* 2003;23:7902–8.